

The Shapes of Dirichlet Defects

Mark Bowick*, Antonio De Felice[†] and Mark Trodden[‡]

Department of Physics, Syracuse University, Syracuse, NY 13244-1130, USA.

Abstract

If the vacuum manifold of a field theory has the appropriate topological structure, the theory admits topological structures analogous to the D-branes of string theory, in which defects of one dimension terminate on other defects of higher dimension. The shapes of such defects are analyzed numerically, with special attention paid to the intersection regions. Walls (co-dimension 1 branes) terminating on other walls, global strings (co-dimension 2 branes) and local strings (including gauge fields) terminating on walls are all considered. Connections to supersymmetric field theories, string theory and condensed matter systems are pointed out.

arXiv:hep-th/0306224v1 23 Jun 2003

* bowick@physics.syr.edu

† defelice@physics.syr.edu

‡ trodden@physics.syr.edu

I. INTRODUCTION.

Topological defects arise whenever spontaneous symmetry breaking leads to a topologically nontrivial manifold of vacua or ground states. Defect configurations involving spatially nonuniform order fields are of considerable interest in any field theory which possesses them as their topological quantum numbers distinguish them from vacua with uniform order fields. A complete understanding of the physical significance of defects requires a good knowledge of their field and energy profile and much effort has been devoted over the years to this subject (see [1, 2] for reviews). Applications range all the way from fundamental physics to cosmology and condensed matter phase transitions.

For a symmetry breaking phase transition $G \rightarrow H$, the vacuum manifold is given by the coset space $\mathcal{M} = G/H$, and p -dimensional defects are classified by the homotopy group $\pi_{d-p-1}(\mathcal{M})$, where d is the spatial dimensionality. For field theories with a relatively simple field content and abelian homotopy groups the associated topological defects are essentially isolated fundamental objects – they do not intersect.

In more complicated field theories new possibilities arise involving composite defects or intersecting arrays of defects. Such configurations add a new layer of mathematical and physical richness. The simplest examples are p -dimensional defects whose boundaries are themselves $(p - 1)$ -dimensional defects [3, 4, 5, 6]. Another example is furnished by theories with non-abelian homotopy groups, such as the quaternionic fundamental group of RP^2 , in which topological defects of a fixed dimension (strings) intersect. Some time ago Carroll and Trodden [7, 8] considered the case of defects which terminate when they intersect defects of equal or higher dimensionality, such as strings ($p = 1$) ending on domain walls ($p = 2$). The defects on which other defects end were termed *Dirichlet topological defects* (DTD), in analogy with D-branes in string theory [9, 10, 11, 12, 13, 14], extended objects on which fundamental strings can terminate. It is important, of course, to keep in mind that there are important differences between the two sets of objects, as emphasized in [7, 15].

Related configurations are of interest in several contexts. Strings terminating on walls can arise in Yang-Mills theories [18, 19, 20, 21] as well as in grand unified models, where they may be of use in tackling the monopole problem [16, 17]. In nonabelian gauge theories, non-intercommuting cosmic strings provide a further example. In addition, in higher spatial dimensions, the required symmetry breaking schemes can lead to a nonabelian unbroken

gauge group, and the phenomenon of confinement for the resulting defects. The rich variety of symmetry breakings and associated ground state manifolds in condensed matter systems provides a particularly concrete context to study topological defects, including the Dirichlet class studied here. In fact an $N = 1$ vortex filament in the nonchiral superfluid ${}^3\text{He} - B$ phase can terminate at a domain wall interface separating this phase from a superfluid ${}^3\text{He} - A$ phase [22], thus realizing a string terminating on a wall.

Since interesting nonlinearities arise both in the cores of such defects and at the points at which distinct classes of defects intersect, it is important to have explicit solutions at hand to study, rather than simply a classification of the associated vacuum structure which guarantees their existence. Some work along these lines has already been performed, particularly in the case of defects networks in supersymmetric theories[44] [28, 29, 30, 31] (for related work in the context of D-branes see [32, 33, 34, 35, 36]). This is the focus of the current paper, whose outline is now provided. In Section II we treat the case of walls ending on walls, followed in Section III by the case of global strings ending on walls. In Section IV we add gauge fields and treat the case of local strings terminating on walls. In each case we give explicit field and energy profiles. Throughout this paper we work in three spatial dimensions.

II. WALLS ENDING ON WALLS

A. The Model

The simplest example of a DTD is a wall ending on another wall. Walls are produced by the spontaneous breaking of discrete symmetries. Consider a theory with three fields, ϕ , ψ_1 and ψ_2 , invariant under three Z_2 symmetries. Such configurations are a special case of Z_n walls [37], and are related to solutions in supersymmetric [38, 39, 40] and supergravity [41, 42] theories.

$$\begin{aligned}
 Z_2^{(1)} &: (\phi \mapsto -\phi, \psi_1 \leftrightarrow \psi_2) \\
 Z_2^{(2)} &: \psi_1 \mapsto -\psi_1 \\
 Z_2^{(3)} &: \psi_2 \mapsto -\psi_2,
 \end{aligned}
 \tag{1}$$

with Lagrangian density [7]

$$\mathcal{L} = \frac{1}{2} \partial_\mu \phi \partial^\mu \phi + \frac{1}{2} \partial_\mu \psi_1 \partial^\mu \psi_1 + \frac{1}{2} \partial_\mu \psi_2 \partial^\mu \psi_2 - V(\phi, \psi_1, \psi_2) , \quad (2)$$

where we choose the most general renormalizable potential invariant under $Z_2^{(1)} \times Z_2^{(2)} \times Z_2^{(3)}$

$$V(\phi, \psi_1, \psi_2) = \lambda_\phi (\phi^2 - \tilde{v}^2)^2 + \lambda_\psi [\psi_1^2 + \psi_2^2 - \tilde{w}^2 + g(\phi^2 - \tilde{v}^2)]^2 + h\psi_1^2\psi_2^2 - \mu\phi(\psi_1^2 - \psi_2^2) . \quad (3)$$

For $\mu = 0$, the minima of V are the 8 points given by

$$\phi = \pm \tilde{v} \quad \text{and} \quad \begin{cases} (\psi_1, \psi_2) = (\pm \tilde{w}, 0) \\ \text{or} \\ (\psi_1, \psi_2) = (0, \pm \tilde{w}) . \end{cases} \quad (4)$$

Since the potential is positive-definite in this case, the presence of h requires either ψ_1 or ψ_2 to vanish, after which the first term in the potential is minimized by $\phi = \pm \tilde{v}$ and the second term by $\psi_1 = \pm \tilde{w}$ or $\psi_2 = \pm \tilde{w}$. For $\mu > 0$ the degeneracy of the 8 vacua is broken, leaving only 4 minima of the potential, at

$$\phi = v, \quad (\psi_1, \psi_2) = (\pm w, 0) ; \quad (5)$$

$$\phi = -v, \quad (\psi_1, \psi_2) = (0, \pm w) , \quad (6)$$

where v is the solution of the cubic equation

$$8\lambda_\phi\lambda_\psi v^3 + 6\lambda_\psi g\mu v^2 - (8\lambda_\phi\lambda_\psi\tilde{v}^2 + \mu^2)v - 2\lambda_\psi\mu(g\tilde{v}^2 + \tilde{w}^2) = 0 , \quad (7)$$

satisfying $\lim_{\mu \rightarrow 0} v = \tilde{v}$, and w is given by

$$w = \left[\tilde{w}^2 + g(\tilde{v}^2 - v^2) + \frac{\mu v}{2\lambda_\psi} \right]^{1/2} . \quad (8)$$

The equations of motion for static fields are then

$$\nabla^2 \phi = 4\lambda_\phi \phi (\phi^2 - \tilde{v}^2) + 4g\lambda_\psi \phi [\psi_1^2 + \psi_2^2 - \tilde{w}^2 + g(\phi^2 - \tilde{v}^2)] - \mu(\psi_1^2 - \psi_2^2) \quad (9)$$

$$\nabla^2 \psi_1 = 4\lambda_\psi \psi_1 [\psi_1^2 + \psi_2^2 - \tilde{w}^2 + g(\phi^2 - \tilde{v}^2)] + 2h\psi_1\psi_2^2 - 2\mu\phi\psi_1 \quad (10)$$

$$\nabla^2 \psi_2 = 4\lambda_\psi \psi_2 [\psi_1^2 + \psi_2^2 - \tilde{w}^2 + g(\phi^2 - \tilde{v}^2)] + 2h\psi_1^2\psi_2 + 2\mu\phi\psi_2 . \quad (11)$$

This model is constructed to admit solutions consisting of domain walls terminating on other domain walls. Such a configuration is intrinsically two-dimensional, and hence is independent of one spatial coordinate, which we choose to be z . What remains is a boundary value problem for an elliptic system of partial differential equations, for which we must prescribe the value of the fields on the boundary.

B. The Numerical Problem - Boundary Conditions

Our choice of boundary conditions is illustrated in Fig. 1, so that we have Dirichlet

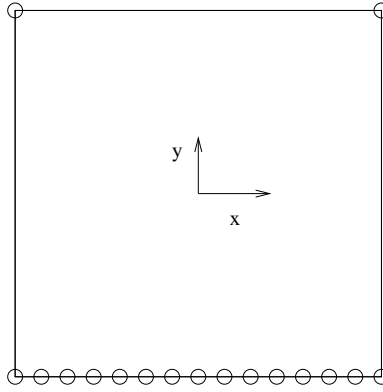


FIG. 1: Boundary conditions for walls on walls. The circles (\circ) represent Dirichlet boundary conditions and solid lines represents Neumann boundary conditions.

boundary conditions

$$\begin{aligned}
 \phi(x, y = -\infty) &= -v , \\
 \psi_1(x, y = -\infty) &= 0 , \\
 \psi_2(x, y = -\infty) &= w ,
 \end{aligned}
 \tag{12}$$

at $y \rightarrow -\infty$, and Neumann boundary conditions everywhere else except at the upper corners, at which we choose

$$\begin{aligned}
 \phi(x = \pm\infty, y = +\infty) &= v , \\
 \psi_1(x = \pm\infty, y = +\infty) &= \pm w , \\
 \psi_2(x = \pm\infty, y = +\infty) &= 0 .
 \end{aligned}
 \tag{13}$$

These choices define a wall in the ψ_1 field, terminating on a wall in the ϕ field – the Dirichlet wall.

The numerical algorithms we use require homogeneous boundary conditions and so we introduce new fields

$$\begin{aligned}\phi &= u_0 + F_0 , \\ \psi_1 &= u_1 + F_1 , \\ \psi_2 &= u_2 + F_2 ,\end{aligned}\tag{14}$$

and define

$$\begin{aligned}F_0(x, y) &= f_{0s}(y) + \frac{1 + \tanh(2y)}{2} [f_{0u}(x) - f_{0s}(y = +\infty)] , \\ F_1(x, y) &= f_{1s}(y) \tanh(2x) + \frac{1 + \tanh(2y)}{2} [f_{1u}(x) - f_{1s}(y = +\infty) \tanh(2x)] , \\ F_2(x, y) &= f_{2s}(y) .\end{aligned}\tag{15}$$

The functions $f_{iu}(x)$ and $f_{is}(y)$ are the solutions of the systems of ordinary differential equations obtained by restricting (9-11) to the “up” boundary ($y = +\infty$) and the “side” boundary ($x = +\infty$) respectively, with $i = 0, 1, 2$ corresponding to ϕ, ψ_1, ψ_2 respectively.

These functions are easily found using standard algorithms with boundary conditions

$$\begin{aligned}f_{0u}(\pm\infty) &= v , \\ f_{1u}(\pm\infty) &= \pm w , \\ f_{2u}(\pm\infty) &= 0 .\end{aligned}\tag{16}$$

$$\begin{aligned}f_{0s}(-\infty) &= -v & f_{0s}(+\infty) &= v \\ f_{1s}(-\infty) &= 0 & f_{1s}(+\infty) &= w \\ f_{2s}(-\infty) &= w & f_{2s}(+\infty) &= 0 .\end{aligned}\tag{17}$$

The symmetries of our problem are such that the solutions on the boundary at $x = -\infty$ are then $\psi_1(x = -\infty, y) = -f_{1s}(y)$ and $\psi_2(x = -\infty, y) = f_{2s}(y)$. Note that one solution $f_{2u}(x) \equiv 0$ is trivial.

We are now in a position to solve numerically our partial differential equations in the

interior. We use a multigrid algorithm [43] to solve for the fields u_i , satisfying

$$\begin{aligned}
 u_i &= 0 && \text{at the } y = -\infty \text{ boundary and at } (x, y) = (\pm\infty, +\infty) , \\
 \partial_x u_i &= 0 && \text{at } x = \pm\infty , \\
 \partial_y u_i &= 0 && \text{at } y = +\infty .
 \end{aligned}
 \tag{18}$$

C. Results - Walls on Dirichlet Walls

We present our results as a set of plots of field profiles and energy densities, providing a number of ways of viewing configuration shapes. We have already defined the field profiles, and the energy density for static fields is given by

$$\begin{aligned}
 E = T^0_0 = -\mathcal{L} &= \frac{1}{2} \left(\frac{\partial\phi}{\partial x} \right)^2 + \frac{1}{2} \left(\frac{\partial\phi}{\partial y} \right)^2 + \frac{1}{2} \left(\frac{\partial\psi_1}{\partial x} \right)^2 + \frac{1}{2} \left(\frac{\partial\psi_1}{\partial y} \right)^2 + \\
 &\frac{1}{2} \left(\frac{\partial\psi_2}{\partial x} \right)^2 + \frac{1}{2} \left(\frac{\partial\psi_2}{\partial y} \right)^2 + V(\phi, \psi_1, \psi_2) .
 \end{aligned}
 \tag{19}$$

The ϕ field domain wall configuration is plotted in Fig. 2. The intersection with the ψ_1 wall at $x = 0$ is clearly visible. The corresponding configuration for ψ_1 is shown in Fig. 3.

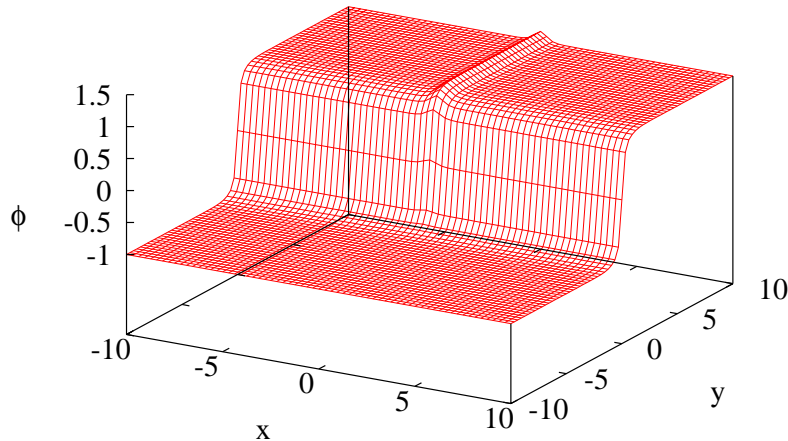


FIG. 2: The ϕ Dirichlet wall configuration.

Note the domain wall for $y = +\infty$. Finally the ψ_2 field configuration is plotted in Fig. 4. It has the form of a wall with half the height of the Dirichlet wall in the sense that it goes

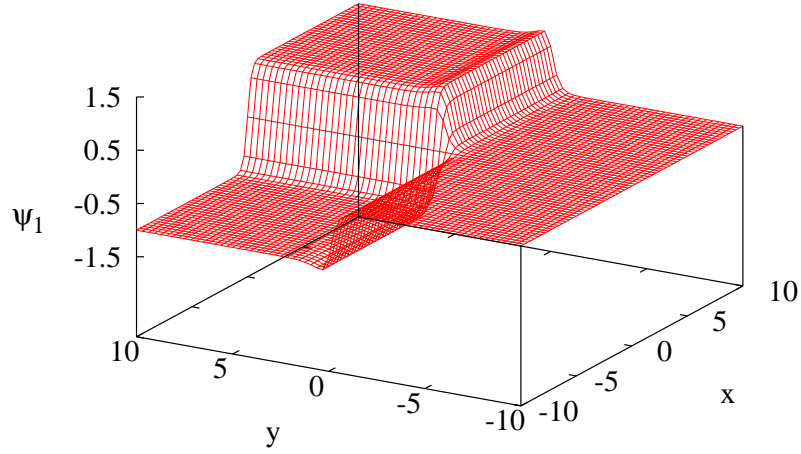


FIG. 3: Field configuration for ψ_1 .

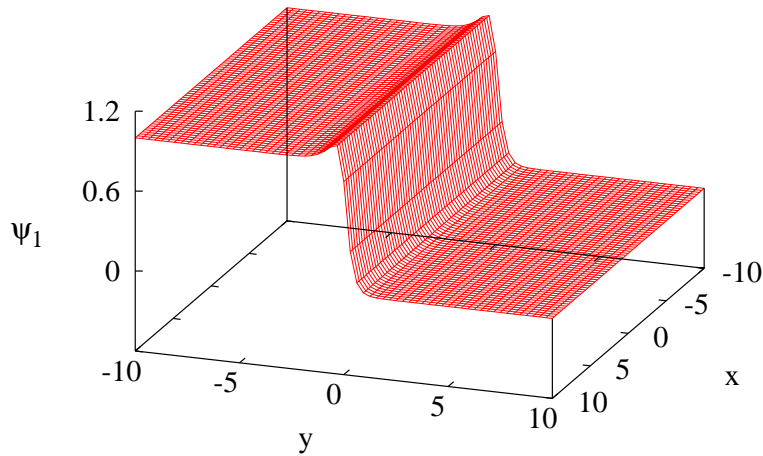


FIG. 4: Walls on walls field configuration for ψ_2 .

from 0 (at $y = +\infty$) to $w = 1$ (at $y = -\infty$). The energy density plotted in Fig. 5 illustrates the merging of the walls at the origin. A corresponding contour plot for the energy density in Fig. 6 shows the wall merging very clearly.

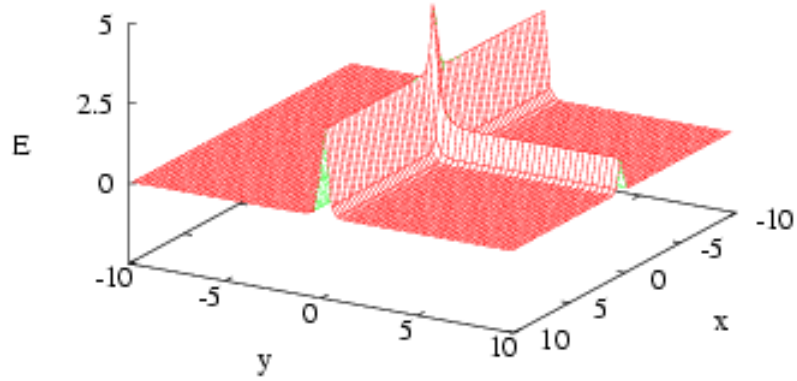


FIG. 5: Energy density for walls ending on walls.

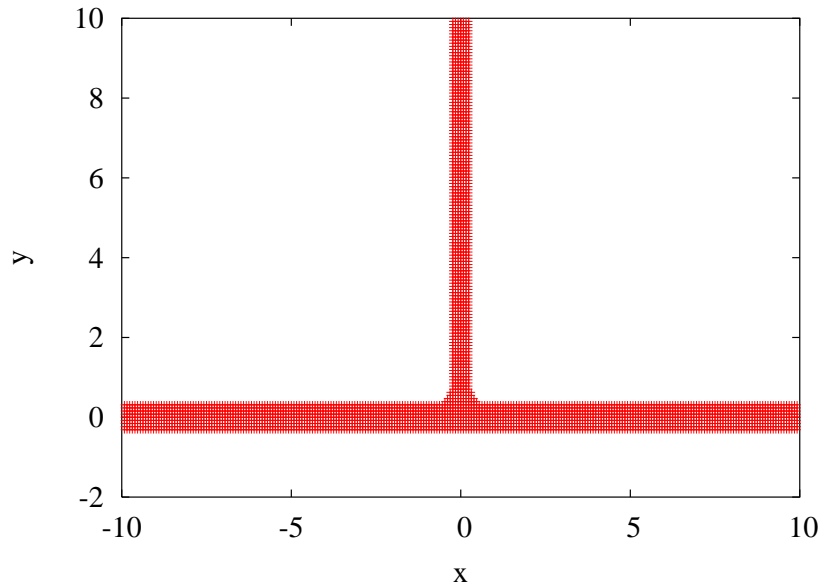


FIG. 6: Contour plot of the energy density for walls ending on walls.

III. GLOBAL STRINGS ENDING ON WALLS

A. The Model

In the simplest case, strings are generated by a breakdown of a $U(1)$ symmetry. In analogy with our approach in the previous section, consider the following transformations

on one real scalar field ϕ and two complex scalar fields ψ_1 and ψ_2 .

$$\begin{aligned} Z_2 &: (\phi \mapsto -\phi, \psi_1 \leftrightarrow \psi_2) \\ U(1)_1 &: \psi_1 \mapsto e^{-i\omega_1} \psi_1 \\ U(1)_2 &: \psi_2 \mapsto e^{-i\omega_2} \psi_2 . \end{aligned} \tag{20}$$

In this section, both $U(1)$ symmetries are global, i.e. ω_i is space-time independent. The Lagrangian density is

$$\mathcal{L} = \frac{1}{2} \partial_\mu \phi \partial^\mu \phi + \partial_\mu \bar{\psi}_1 \partial^\mu \psi_1 + \partial_\mu \bar{\psi}_2 \partial^\mu \psi_2 - V(\phi, \psi_1, \psi_2) , \tag{21}$$

with potential

$$\begin{aligned} V(\phi, \psi_1, \psi_2) &= \lambda_\phi (\phi^2 - \tilde{v}^2)^2 + \lambda_\psi [|\psi_1|^2 + |\psi_2|^2 - \tilde{w}^2 + g(\phi^2 - \tilde{v}^2)]^2 \\ &+ h|\psi_1|^2|\psi_2|^2 - \mu\phi(|\psi_1|^2 - |\psi_2|^2) . \end{aligned} \tag{22}$$

Consider the following static ansatz

$$\begin{aligned} \phi &= \phi(r, z) \\ \psi_1 &= R_1(r, z) e^{i\theta} \\ \psi_2 &= \psi_2(r, z) , \end{aligned} \tag{23}$$

where ϕ , R_1 and ψ_2 are real functions, for which the equations of motion are

$$\nabla^2 \phi = 4\lambda_\phi \phi (\phi^2 - \tilde{v}^2) + 4\lambda_\psi g \phi [R_1^2 + \psi_2^2 - \tilde{w}^2 + g(\phi^2 - \tilde{v}^2)] - \mu(R_1^2 - \psi_2^2) , \tag{24}$$

$$\nabla^2 R_1 = 2\lambda_\psi R_1 [R_1^2 + \psi_2^2 - \tilde{w}^2 + g(\phi^2 - \tilde{v}^2)] + hR_1 \psi_2^2 - \mu\phi R_1 , \tag{25}$$

$$\nabla^2 \psi_2 = 2\lambda_\psi \psi_2 [R_1^2 + \psi_2^2 - \tilde{w}^2 + g(\phi^2 - \tilde{v}^2)] + hR_1^2 \psi_2 + \mu\phi \psi_2 . \tag{26}$$

B. The Numerical Problem - Boundary Conditions

We now proceed as in the previous section, imposing the boundary conditions illustrated in Fig. 7.

We choose Dirichlet boundary conditions for the bottom boundary

$$\begin{aligned} \phi(r, z = -\infty) &= -v , \\ R_1(r, z = -\infty) &= 0 , \\ \psi_2(r, z = -\infty) &= w , \end{aligned} \tag{27}$$

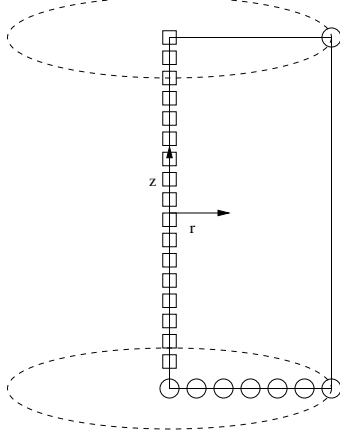


FIG. 7: Boundary conditions for a string ending on a wall. The circles (\circ) represent Dirichlet boundary conditions, the squares (\square) represent mixed boundary conditions (Dirichlet for some fields, Neumann for the remaining ones) and solid lines represent Neumann boundary conditions.

and at the upper corner we impose

$$\begin{aligned}
 \phi(r = \infty, z = +\infty) &= v , \\
 R_1(r = \infty, z = +\infty) &= w , \\
 \psi_2(r = \infty, z = +\infty) &= 0 .
 \end{aligned}
 \tag{28}$$

The boundary $r = 0$ requires a more detailed discussion. Taylor expanding the fields around $r = 0$, we have

$$\phi = \sum_n a_n(z) r^n , \quad R_1 = \sum_n b_n(z) r^n , \quad \psi_2 = \sum_n c_n(z) r^n .
 \tag{29}$$

Equations [24-26], in the limit $r \rightarrow 0$, become

$$\begin{aligned}
 \frac{a_1(z)}{r} + 4a_2(z) + \frac{d^2 a_0(z)}{dz^2} &= f_0[a_0(z), b_0(z), c_0(z)] , \\
 3b_2(z) - \frac{b_0(z)}{r^2} + \frac{d^2 b_0(z)}{dz^2} &= f_1[a_0(z), b_0(z), c_0(z)] , \\
 \frac{c_1(z)}{r} + 4c_2(z) + \frac{d^2 c_0(z)}{dz^2} &= f_2[a_0(z), b_0(z), c_0(z)] .
 \end{aligned}
 \tag{30}$$

Demanding regularity at the origin gives

$$\begin{aligned}
 a_1(z) = 0 \quad \partial_r \phi|_{r=0} &= 0 , \\
 b_0(z) = 0 \quad R_1|_{r=0} &= 0 , \\
 c_1(z) = 0 \quad \partial_r \psi_2|_{r=0} &= 0 .
 \end{aligned}
 \tag{31}$$

For the other boundaries we imposed Neumann boundary conditions for all the fields.

As for the case of walls on walls, we define new fields with homogeneous boundary conditions. Defining the “up” boundary to be at $z = +\infty$ and the “side” boundary to be at $r = +\infty$ we again introduce the functions $f_{iu}(r)$ and $f_{is}(z)$ which are solutions to the appropriate systems of ordinary differential equations with boundary conditions

$$\begin{aligned} \partial_r f_{0u}(0) &= 0 & f_{0u}(+\infty) &= v , \\ f_{1u}(0) &= 0 & f_{1u}(+\infty) &= w , \\ \partial_r f_{2u}(0) &= 0 & f_{2u}(+\infty) &= 0 , \end{aligned} \tag{32}$$

$$\begin{aligned} f_{0s}(-\infty) &= -v & f_{0s}(+\infty) &= v , \\ f_{1s}(-\infty) &= 0 & f_{1s}(+\infty) &= w , \\ f_{2s}(-\infty) &= w & f_{2s}(+\infty) &= 0 . \end{aligned} \tag{33}$$

Again we have a trivial solution $f_{2u}(r) \equiv 0$. Following the previous section, we define the following functions

$$\begin{aligned} F_0(r, z) &= f_{0s}(z) + \frac{1 + \tanh(2z)}{2} [f_{0u}(r) - f_{0s}(z = +\infty)] , \\ F_1(r, z) &= f_{1s}(z) \tanh(r) + \frac{1 + \tanh(2z)}{2} [f_{1u}(r) - f_{1s}(z = +\infty) \tanh(r)] , \\ F_2(r, z) &= f_{2s}(z) , \end{aligned} \tag{34}$$

and introduce new fields

$$\begin{aligned} \phi &= u_0 + F_0 , \\ \psi_1 &= u_1 + F_1 , \\ \psi_2 &= u_2 + F_2 , \end{aligned} \tag{35}$$

obeying homogeneous boundary conditions

$$\begin{aligned} u_i &= 0 & \text{at the } z = -\infty \text{ boundary, at } (r, z) = (+\infty, +\infty) \\ & & \text{and for } u_1 \text{ at the core of the string,} \\ \partial_r u_i &= 0 & \text{at the } r = +\infty \text{ boundary and for } i = 0, 2 \text{ at the core of the string,} \\ \partial_z u_i &= 0 & \text{at the } z = +\infty \text{ boundary .} \end{aligned}$$

C. Results - Global Strings Ending on Dirichlet Walls

To help in understanding our plots, note that the energy density for static fields in this section is given by

$$E = T^0_0 = -\mathcal{L} = \frac{1}{2} \left(\frac{\partial\phi}{\partial r} \right)^2 + \frac{1}{2} \left(\frac{\partial\phi}{\partial z} \right)^2 + \left(\frac{\partial\psi_2}{\partial r} \right)^2 + \left(\frac{\partial\psi_2}{\partial z} \right)^2 + \left(\frac{\partial R_1}{\partial r} \right)^2 + \frac{R_1^2}{r^2} + \left(\frac{\partial R_1}{\partial z} \right)^2 + V(\phi, R_1, \psi_2). \quad (36)$$

The ϕ field domain wall configuration is plotted in Fig. 8. The intersection with the ψ_1 string at $r = 0$ is clearly visible. The corresponding configuration for ψ_1 is shown in Fig. 9.

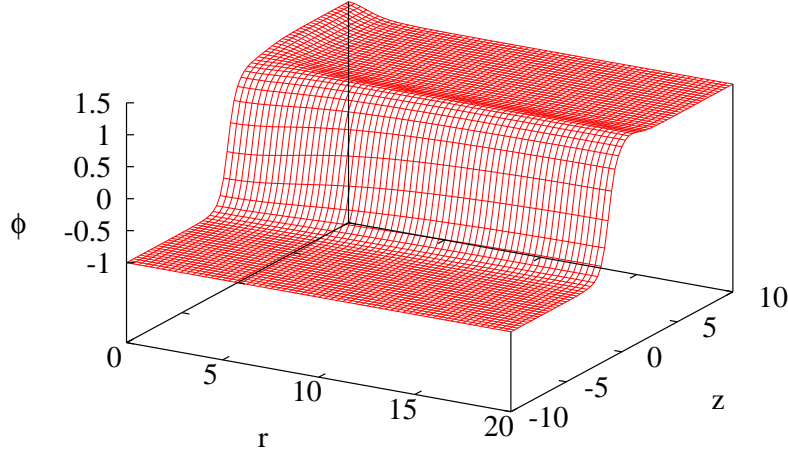


FIG. 8: Field ϕ , the Dirichlet wall.

Note the string for $z = +\infty$. Finally the ψ_2 field configuration is plotted in Fig. 10. It has the form of a wall (except for an interaction with the string for $r = 0$ and $z > 0$) with half the height of the Dirichlet wall in the sense that it goes from 0 (at $z = +\infty$) to $w = 1$ (at $z = -\infty$).

The energy density plotted in Fig. 11 illustrates the merging of the string with the wall at the origin. A corresponding contour plot for the energy density in Fig. 12 shows the string ending on the wall very clearly.

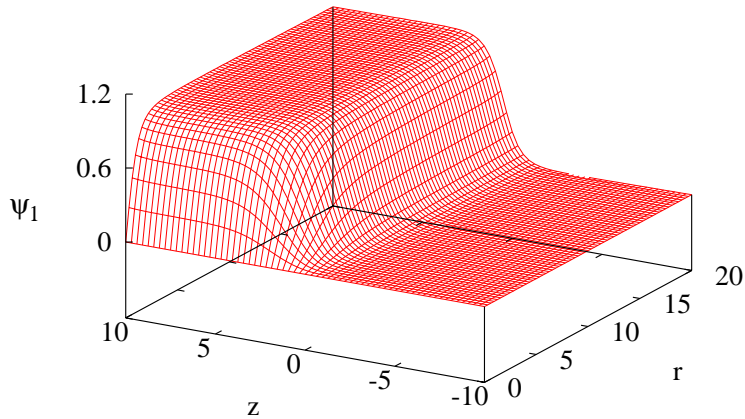


FIG. 9: Field ψ_1 , the global string.

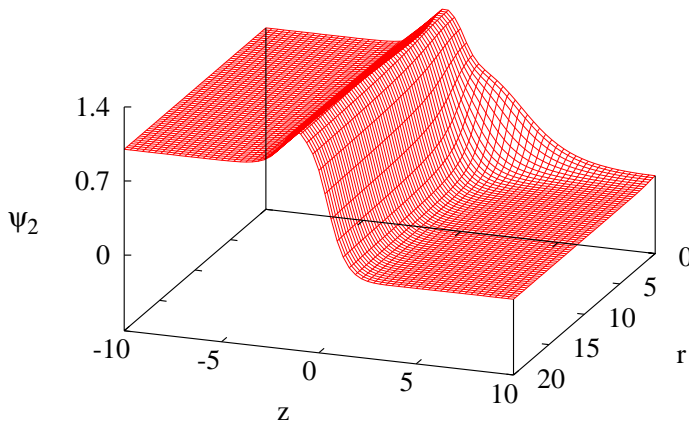


FIG. 10: Field ψ_2 for a global string and a wall.

IV. GAUGE STRINGS ON WALLS

More interesting connections with physical models can be made by introducing gauge fields. In this section we take the first steps towards this by finding numerical solutions for local cosmic strings terminating on Dirichlet domain walls.

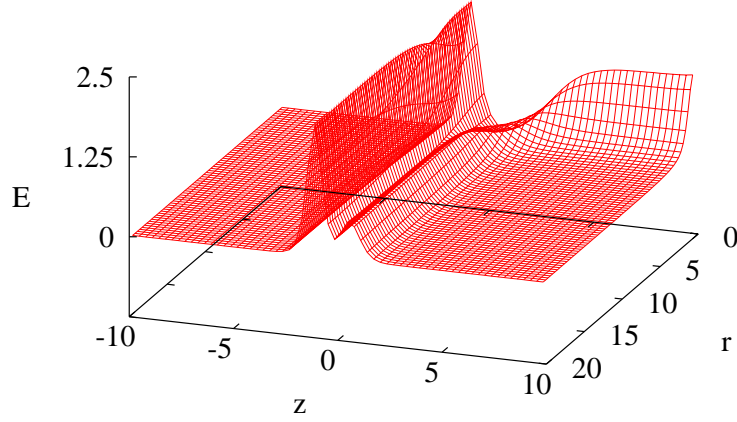


FIG. 11: Energy density for a global string ending on a wall.

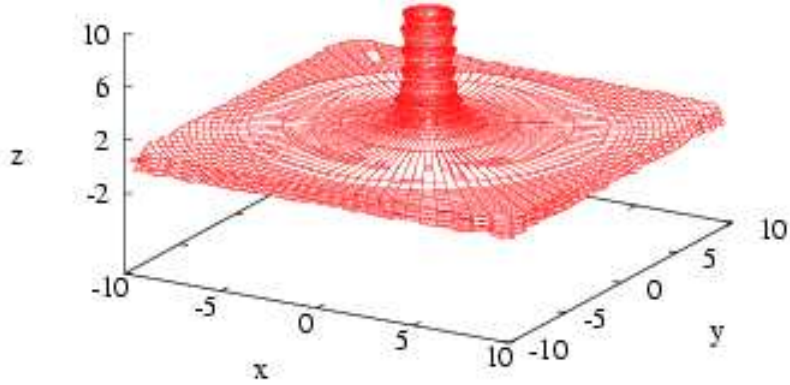


FIG. 12: Contour plot of the energy density for a global string ending on a wall.

V. THE MODEL

We modify the Lagrangian density of the last section by introducing a $U(1)$ gauge field A_μ , under which the field ψ_1 is charged.

$$\mathcal{L} = \frac{1}{2} \partial_\mu \phi \partial^\mu \phi + \bar{D}_\mu \bar{\psi}_1 D^\mu \psi_1 + \partial_\mu \bar{\psi}_2 \partial^\mu \psi_2 - \frac{1}{4} F^{\mu\nu} F_{\mu\nu} - V(\phi, \psi_1, \psi_2) , \quad (37)$$

where

$$D_\mu = \partial_\mu - ieA_\mu . \quad (38)$$

The equations of motion for ϕ and ψ_2 are unchanged from the case of the global string, since we have constructed the model so that the relevant winding occurs for the ψ_1 field only. Thus, the modified equation of motion for ψ_1 is

$$\partial_\mu \partial^\mu \psi_1 - ie \partial_\mu (A^\mu \psi_1) + \frac{\partial V}{\partial \psi_1} - ie A_\mu (\partial^\mu \psi_1 - ie A^\mu \psi_1) = 0 . \quad (39)$$

Imposing the Lorentz condition $\partial_\mu A^\mu = 0$ for a static gauge field yields

$$\vec{\nabla} \cdot \vec{A} = 0 , \quad (40)$$

and equation (39) then becomes

$$\nabla^2 \psi_1 = \frac{\partial V}{\partial \psi_1} - 2ie \vec{A} \cdot \vec{\nabla} \psi_1 + e^2 (\vec{A} \cdot \vec{A}) \psi_1 . \quad (41)$$

We are interested in the ansatz

$$\begin{aligned} \phi &= \phi(r, z) , \\ \psi_1 &= R_1(r, z) e^{i\theta} , \\ \psi_2 &= \psi_2(r, z) , \end{aligned} \quad (42)$$

where ϕ , R_1 and ψ_2 are real functions. As is well known for cosmic strings, the imaginary part of equation (41) gives

$$A_r \frac{\partial R_1}{\partial r} + A_z \frac{\partial R_1}{\partial z} = 0 , \quad (43)$$

with solution

$$\vec{A} = A \hat{\theta} , \quad (44)$$

so that the Lorentz condition becomes $\partial_\theta A = 0$. The equation for R_1 then becomes

$$\begin{aligned} \nabla^2 R_1 &= \frac{\partial^2 R_1}{\partial r^2} + \frac{1}{r} \frac{\partial R_1}{\partial r} - \frac{R_1}{r^2} + \frac{\partial^2 R_1}{\partial z^2} = \\ &= 2\lambda_\psi R_1 [R_1^2 + \psi_2^2 - \tilde{w}^2 + g(\phi^2 - \tilde{v}^2)] + h R_1 \psi_2^2 - \mu \phi R_1 + 2e \frac{A R_1}{r} + e^2 A^2 R_1 , \end{aligned} \quad (45)$$

and the equation for the gauge field is

$$\square A^\alpha = j^\alpha = 2e \text{Im}[\bar{\psi}_1 (\partial^\alpha - ie A^\alpha) \psi_1] , \quad (46)$$

which, for our ansatz, is

$$(\vec{\nabla}^2 \vec{A})_\theta = 2e R_1^2 (r^{-1} + eA) . \quad (47)$$

A. The Numerical Problem - Boundary Conditions

The geometry of the problem is identical to that for global strings, and so we refer the reader again to Fig. 7. We choose Dirichlet boundary conditions for the bottom boundary

$$\begin{aligned}
\phi(r, z = -\infty) &= -v , \\
R_1(r, z = -\infty) &= 0 , \\
\psi_2(r, y = -\infty) &= w , \\
A(r, y = -\infty) &= 0 ,
\end{aligned}
\tag{48}$$

and at the upper corner

$$\begin{aligned}
\phi(r = \infty, z = +\infty) &= v , \\
R_1(r = \infty, z = +\infty) &= w , \\
\psi_2(r = \infty, z = +\infty) &= 0 , \\
A(r = \infty, z = +\infty) &= 0 .
\end{aligned}
\tag{49}$$

At the core of the string we choose

$$\begin{aligned}
\partial_r \phi(r = 0, z) &= \partial_r \psi_2(r = 0, z) = 0 , \\
R_1(r = 0, z) &= A(r = 0, z) = 0 ,
\end{aligned}
\tag{50}$$

and for the boundary at $r = +\infty$ we impose Neumann conditions for all the fields. The choice of these boundary conditions defines a string ending on a Dirichlet wall.

We again solve ordinary differential equations on the boundaries at $z = +\infty$ and $r = +\infty$. We keep the same notation as in the previous section, but now include the gauge field A by defining $f_{3u}(r)$ and $f_{3s}(z)$ with boundary conditions

$$f_{3u}(0) = 0 \quad \partial_r f_{3u}(+\infty) = 0 , \tag{51}$$

$$f_{3s}(-\infty) = 0 \quad f_{3s}(+\infty) = 0 . \tag{52}$$

Once again $f_{2u}(r) \equiv 0$ and $f_{3s}(z) \equiv 0$ are trivial solutions.

As before we define

$$\begin{aligned}
F_0(r, z) &= f_{0s}(z) + \frac{1 + \tanh(2z)}{2} [f_{0u}(r) - f_{0s}(z = +\infty)] , \\
F_1(r, z) &= f_{1s}(z) \tanh(r) + \frac{1 + \tanh(2z)}{2} [f_{1u}(r) - f_{1s}(z = +\infty) \tanh(r)] , \\
F_2(r, z) &= f_{2s}(z) , \\
F_3(r, z) &= \frac{1 + \tanh(2z)}{2} f_{3u}(r) ,
\end{aligned} \tag{53}$$

and new fields

$$\begin{aligned}
\phi &= u_0 + F_0 , \\
\psi_1 &= u_1 + F_1 , \\
\psi_2 &= u_2 + F_2 , \\
A &= u_3 + F_3 ,
\end{aligned} \tag{54}$$

with homogeneous boundary conditions

$$\begin{aligned}
u_i = 0 & \quad \text{at the } z = -\infty \text{ boundary, at the corner } (r, z) = (+\infty, +\infty) \\
& \quad \text{and, for } i = 1, 3, \text{ at the core of the string,} \\
\partial_r u_i = 0 & \quad \text{at the } r = +\infty \text{ boundary and, for } i = 0, 2, \text{ at the core of the string,} \\
\partial_z u_i = 0 & \quad \text{at the } z = +\infty \text{ boundary .}
\end{aligned}$$

B. Results - Local Strings Ending on Dirichlet Walls

We plot our results as before, with the energy density now given by

$$\begin{aligned}
E = T^0_0 = -\mathcal{L} &= \frac{1}{2} \left(\frac{\partial \phi}{\partial r} \right)^2 + \frac{1}{2} \left(\frac{\partial \phi}{\partial z} \right)^2 + \left(\frac{\partial \psi_2}{\partial r} \right)^2 + \left(\frac{\partial \psi_2}{\partial z} \right)^2 + \\
& \quad \left(\frac{\partial R_1}{\partial r} \right)^2 + R_1^2 \left(\frac{1}{r} + eA \right)^2 + \left(\frac{\partial R_1}{\partial z} \right)^2 + \frac{1}{2} \vec{B}^2 + V(\phi, R_1, \psi_2) .
\end{aligned} \tag{55}$$

We also plot the magnetic field associated with the gauge field of the string, given by

$$\vec{B} = -\frac{\partial A}{\partial z} \hat{r} + \frac{1}{r} \frac{\partial(rA)}{\partial r} \hat{z} . \tag{56}$$

The ϕ field domain wall configuration is plotted in Fig. 13. The intersection with the ψ_1 string at $r = 0$ is clearly visible. The corresponding configuration for ψ_1 is shown in Fig. 14. Note the string for $z = +\infty$. The field ψ_2 configuration is plotted in Fig. 15. It has the form

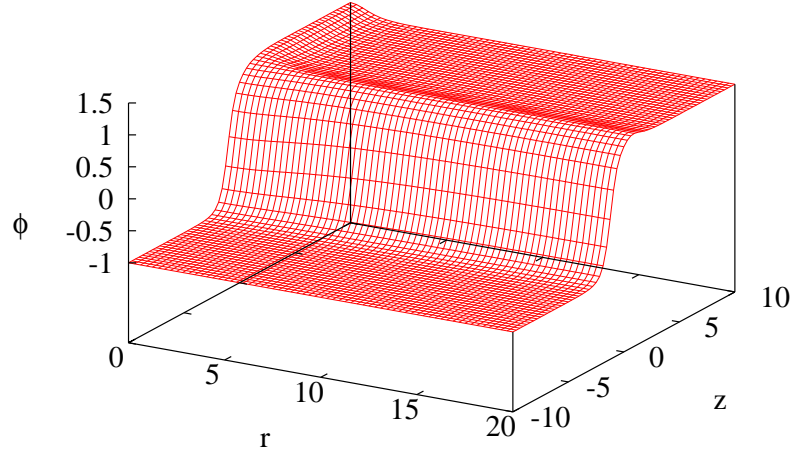


FIG. 13: The ϕ field configuration: Dirichlet wall for local strings.

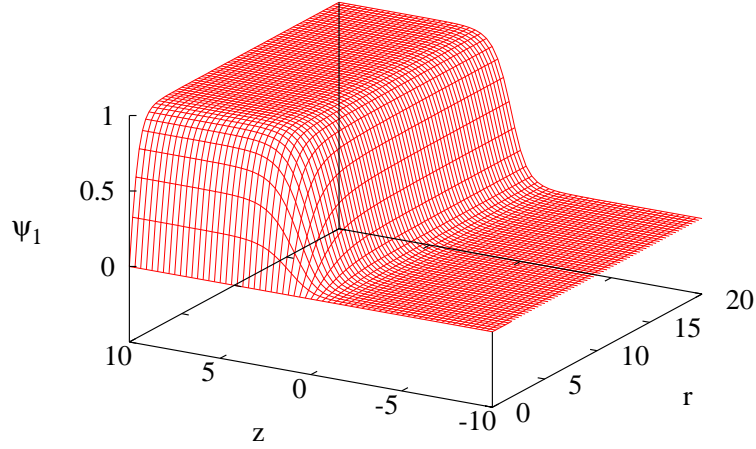


FIG. 14: The local string field ψ_1 .

of a wall (except for an interaction with the string for $r = 0$ and $z > 0$) with half the height of the Dirichlet wall in the sense that it goes from 0 (at $z = +\infty$) to $w = 1$ (at $z = -\infty$). Finally the gauge field configuration is shown in Fig. 16. We can verify that $A \rightarrow r^{-1}$ as $(r, z) \rightarrow +\infty$. We plotted the r component of the magnetic field, B_r , in Fig. 17. The z component of the magnetic field, B_z , is illustrated in Fig. 18 A 2-D plot of the vector field

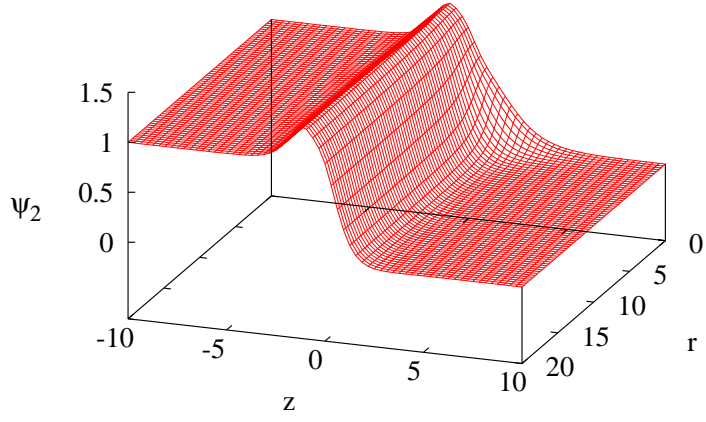


FIG. 15: Field configuration ψ_2 for a local string ending on a wall.

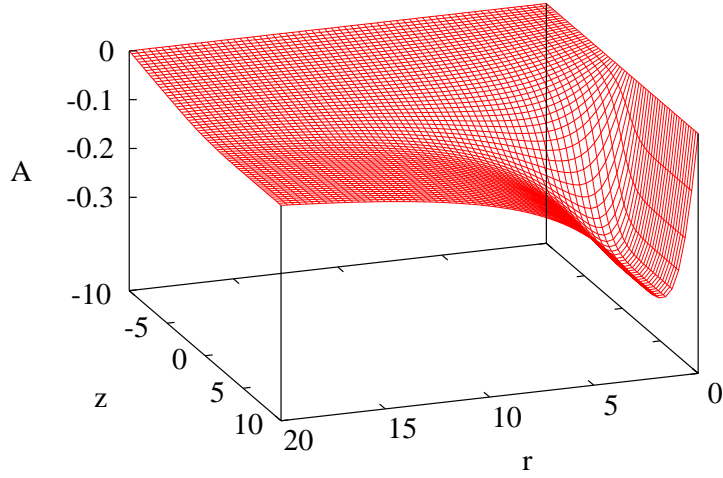


FIG. 16: The gauge field A.

\vec{B} is shown in Fig. 19. The energy density plotted in Fig. 20 illustrates the string merging at the origin with the Dirichlet wall. A corresponding contour plot of the energy density in Fig. 21 shows the string ending on the wall very clearly.

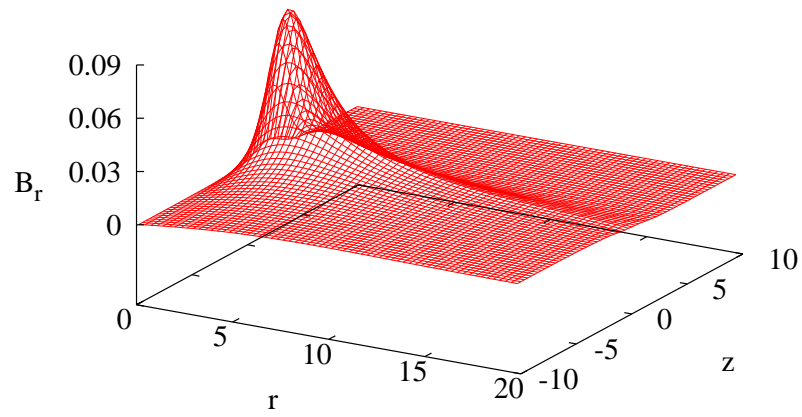


FIG. 17: Component B_r of the magnetic field.

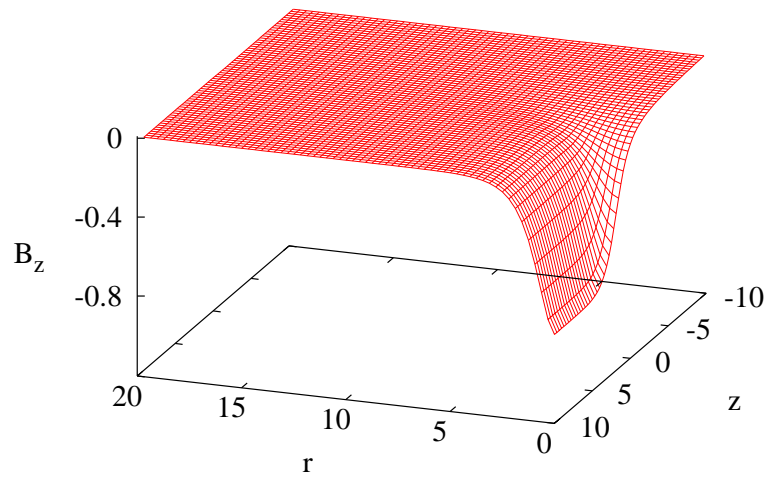


FIG. 18: Component B_z of the magnetic field.

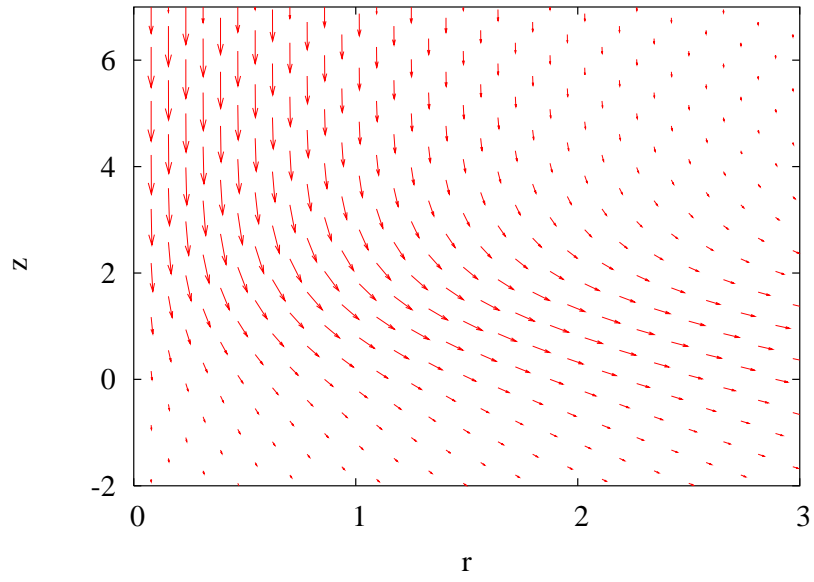


FIG. 19: 2D plot of the magnetic field \vec{B} .

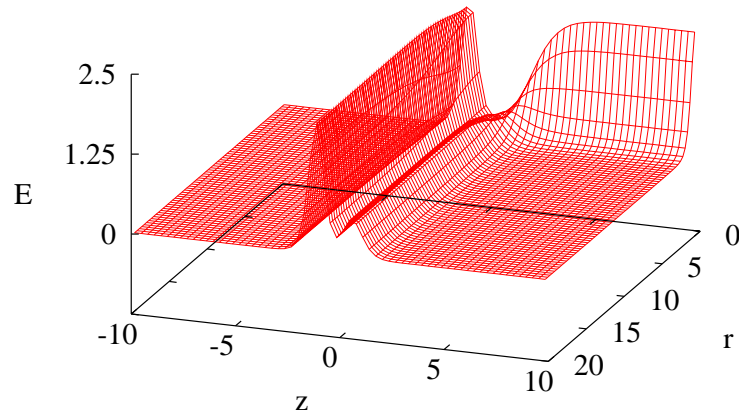


FIG. 20: Energy density for a local string ending on a wall.

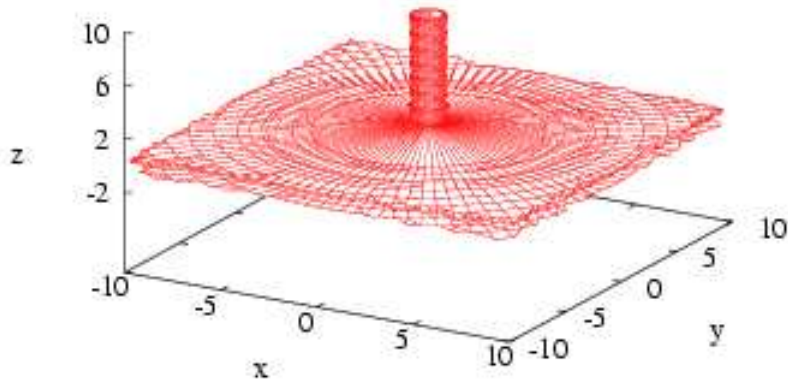


FIG. 21: Contour plot for the energy density for a local string ending on a wall.

Acknowledgments

We thank Joel Rozowsky for helpful discussions. MB is supported by the US Department of Energy (DOE) under contract No. DE-FG02-85ER40237 and by the National Science Foundation (NSF) under grant DMR-0219292. ADF and MT are supported in part by the NSF under grant PHY-0094122. MT is a Cottrell Scholar of Research Corporation.

-
- [1] A. Vilenkin and E.P.S. Shellard, *Cosmic Strings and Other Topological Defects*, Cambridge University Press (1994).
 - [2] M. B. Hindmarsh and T. W. Kibble, Rept. Prog. Phys. **58**, 477 (1995) [arXiv:hep-ph/9411342].
 - [3] T. W. Kibble, G. Lazarides and Q. Shafi, Phys. Rev. D **26**, 435 (1982).
 - [4] A. Vilenkin, Nucl. Phys. B **196**, 240 (1982).
 - [5] M. Hindmarsh and T. W. Kibble, Phys. Rev. Lett. **55**, 2398 (1985).
 - [6] A. Chamblin and D. M. Eardley, Phys. Lett. B **475**, 46 (2000) [arXiv:hep-th/9912166].
 - [7] S. M. Carroll and M. Trodden, Phys. Rev. D **57**, 5189 (1998) [arXiv:hep-th/9711099].
 - [8] M. Trodden, arXiv:hep-th/9901062.
 - [9] P. Horava, Nucl. Phys. B **327**, 461 (1989).

- [10] P. Horava, Phys. Lett. B **231**, 251 (1989).
- [11] J. Dai, R. G. Leigh and J. Polchinski, Mod. Phys. Lett. A **4**, 2073 (1989).
- [12] J. Polchinski, Phys. Rev. Lett. **75**, 4724 (1995) [arXiv:hep-th/9510017].
- [13] J. Polchinski, S. Chaudhuri and C. V. Johnson, arXiv:hep-th/9602052.
- [14] J. Polchinski, arXiv:hep-th/9611050.
- [15] G. Dvali and A. Vilenkin, Phys. Rev. D **67**, 046002 (2003) [arXiv:hep-th/0209217].
- [16] G. R. Dvali, H. Liu and T. Vachaspati, Phys. Rev. Lett. **80**, 2281 (1998) [arXiv:hep-ph/9710301].
- [17] S. Alexander, R. H. Brandenberger, R. Easther and A. Sornborger, arXiv:hep-ph/9903254.
- [18] E. Witten, Nucl. Phys. B **507**, 658 (1997) [arXiv:hep-th/9706109].
- [19] A. Campos, K. Holland and U. J. Wiese, Phys. Rev. Lett. **81**, 2420 (1998) [arXiv:hep-th/9805086].
- [20] K. Holland and U. J. Wiese, arXiv:hep-ph/0011193.
- [21] G. R. Dvali, G. Gabadadze and Z. Kakushadze, Nucl. Phys. B **562**, 158 (1999) [arXiv:hep-th/9901032].
- [22] G. E. Volovik, Proc. Nat. Acad. Sci. **97**, 2431 (2000) [arXiv:cond-mat/9911486].
- [23] S. C. Davis, A. C. Davis and M. Trodden, Phys. Lett. B **405**, 257 (1997) [arXiv:hep-ph/9702360].
- [24] S. C. Davis, A. C. Davis and M. Trodden, Phys. Rev. D **57**, 5184 (1998) [arXiv:hep-ph/9711313].
- [25] J. R. Morris, Phys. Rev. D **52**, 1096 (1995).
- [26] J. R. Morris, Model,” Phys. Rev. D **53**, 2078 (1996) [arXiv:hep-ph/9511293].
- [27] J. R. Morris, Phys. Rev. D **56**, 2378 (1997) [arXiv:hep-ph/9706302].
- [28] D. Bazeia, H. Boschi-Filho and F. A. Brito, JHEP **9904**, 028 (1999) [arXiv:hep-th/9811084].
- [29] P. M. Saffin, Phys. Rev. Lett. **83**, 4249 (1999) [arXiv:hep-th/9907066].
- [30] D. Bazeia and F. A. Brito, Phys. Rev. D **61**, 105019 (2000) [arXiv:hep-th/9912015].
- [31] D. Bazeia, F. A. Brito, W. Freire and R. F. Ribeiro, arXiv:hep-th/0210289.
- [32] E. Witten, Nucl. Phys. B **500**, 3 (1997) [arXiv:hep-th/9703166].
- [33] C. G. Callan and J. M. Maldacena, Nucl. Phys. B **513**, 198 (1998) [arXiv:hep-th/9708147].
- [34] G. W. Gibbons, Nucl. Phys. B **514**, 603 (1998) [arXiv:hep-th/9709027].
- [35] P. S. Howe, N. D. Lambert and P. C. West, Nucl. Phys. B **515**, 203 (1998)

- [arXiv:hep-th/9709014].
- [36] A. Hashimoto, Phys. Rev. D **57**, 6441 (1998) [arXiv:hep-th/9711097].
- [37] B. S. Ryden, W. H. Press and D. N. Spergel, Ap. J. **357**, 293 (1990).
- [38] G. W. Gibbons and P. K. Townsend, Phys. Rev. Lett. **83**, 1727 (1999) [arXiv:hep-th/9905196].
- [39] S. M. Carroll, S. Hellerman and M. Trodden, Phys. Rev. D **61**, 065001 (2000) [arXiv:hep-th/9905217].
- [40] J. P. Gauntlett, R. Portugues, D. Tong and P. K. Townsend, Phys. Rev. D **63**, 085002 (2001) [arXiv:hep-th/0008221].
- [41] S. M. Carroll, S. Hellerman and M. Trodden, Phys. Rev. D **62**, 044049 (2000) [arXiv:hep-th/9911083].
- [42] A. Hashimoto, JHEP **9901**, 018 (1999) [arXiv:hep-th/9812159].
- [43] U. Trottenberg, C. Oosterlee, and A. Schüller, *Multigrid*, (Academic Press, San Diego, 2001).
- [44] For microphysical properties of defects in supersymmetric theories see [23, 24, 25, 26, 27].